

Spin dynamics and magnetic order in magnetically frustrated $\text{Tb}_2\text{Sn}_2\text{O}_7$

P. Dalmas de Réotier,¹ A. Yaouanc,¹ L. Keller,² A. Cervellino,^{2,*} B. Roessli,²
C. Baines,³ A. Forget,⁴ C. Vaju,¹ P.C.M. Gubbens,⁵ A. Amato,⁶ and P.J.C. King⁷

¹CEA/DSM/Département de Recherche Fondamentale sur la Matière Condensée, 38054 Grenoble, France

²Laboratory for Neutron Scattering, ETH Zürich and Paul Scherrer Institute, 5232 Villigen-PSI, Switzerland

³Low temperature facilities group, Paul Scherrer Institute, 5232 Villigen-PSI, Switzerland

⁴CEA/DSM/Département de Recherche sur l'Etat Condensée,
les Atomes et les Molécules, 91191 Gif sur Yvette, France

⁵Department of Radiation, Radionuclides & Reactors,
Delft University of Technology, 2629 JB Delft, The Netherlands

⁶Laboratory for Muon-Spin Spectroscopy, Paul Scherrer Institute, 5232 Villigen-PSI, Switzerland

⁷ISIS Facility, Rutherford Appleton Laboratory, Chilton, Didcot, OX11 0QX, UK

(Dated: June 23, 2021)

We report a study of the geometrically frustrated magnetic material $\text{Tb}_2\text{Sn}_2\text{O}_7$ by the positive muon spin relaxation technique. No signature of a static magnetically ordered state is detected while neutron magnetic reflections are observed in agreement with a published report. This is explained by the dynamical nature of the ground state of $\text{Tb}_2\text{Sn}_2\text{O}_7$: the Tb^{3+} magnetic moment characteristic fluctuation time is $\simeq 10^{-10}$ s. The strong effect of the magnetic field on the muon spin-lattice relaxation rate at low fields indicates a large field-induced increase of the magnetic density of states of the collective excitations at low energy.

PACS numbers: 75.40.-s, 75.25.+z, 76.75.+i

Magnetic materials with antiferromagnetically coupled spins located on triangular motifs exhibit geometrical magnetic frustration because their spatial arrangement is such that it prevents the simultaneous minimization of all the interaction energies [1]. The frustration, which leads to a highly degenerate ground state, forbids magnetic order to occur. Perturbations to the nearest-neighbor exchange interaction, such as exchange interactions extending beyond nearest-neighbor magnetic atoms, dipole coupling or magnetic anisotropy, are believed to be responsible for the magnetic order observed in some compounds [2]. Typical examples are given by the spinel structure oxide LiMn_2O_4 , the pyrochlore structure compounds $\text{Gd}_2\text{Ti}_2\text{O}_7$, $\text{Er}_2\text{Ti}_2\text{O}_7$, $\text{Tb}_2\text{Sn}_2\text{O}_7$ and $\text{Gd}_2\text{Sn}_2\text{O}_7$ and the cuprate mineral $\text{Cu}_2\text{Cl}(\text{OH})_3$. According to neutron diffraction (ND) measurements, long- and short-range orders coexist in LiMn_2O_4 [3], a partial order of the Gd^{3+} magnetic moments is established at low temperature in $\text{Gd}_2\text{Ti}_2\text{O}_7$ [4] and a conventional magnetic order exists for the last three pyrochlore compounds [5, 6, 7]. When looked for, persistent spin dynamics has always been found far below the magnetic ordering temperature. The possibility of such dynamics is conceivable for the partly ordered structure of $\text{Gd}_2\text{Ti}_2\text{O}_7$ [8] and $\text{Cu}_2\text{Cl}(\text{OH})_3$ [9] but more exotic when all the magnetic moments contribute to the magnetic structure as for $\text{Er}_2\text{Ti}_2\text{O}_7$ [10], $\text{Gd}_2\text{Sn}_2\text{O}_7$ [11, 12] and $\text{Tb}_2\text{Sn}_2\text{O}_7$ [6]. A prerequisite for understanding the unanticipated behavior of these latter systems is a careful characterization of their dynamical properties.

Here we show that positive muon spin relaxation (μSR) and ND results in the ordered phase of $\text{Tb}_2\text{Sn}_2\text{O}_7$ can be simultaneously accounted for only if the Tb^{3+} moments

are strongly dynamical. An independent and consistent time scale is obtained from a careful analysis of the neutron data. In addition, the initial strong and counter-intuitive increase of the muon relaxation rate when a magnetic field is applied indicates an increase of the density of magnetic excitations at very low energy.

$\text{Tb}_2\text{Sn}_2\text{O}_7$ crystallizes with the cubic space group $Fd\bar{3}m$. Rietveld refinements of powder x-ray and ND patterns yield the lattice constant $a = 10.426$ Å and the free position parameter allowed by the space group for the $48f$ site occupied by oxygen, $x = 0.336$ [6]. Magnetic measurements point to a magnetic transition at 0.87 K and to strong antiferromagnetic interactions as deduced from the large and negative Curie-Weiss constant $\theta_{\text{CW}} = -12$ K [13]. Powder ND indicates a structure with both ferromagnetic and antiferromagnetic components below $T_{\text{sr}} = 1.3$ (1) K where short-range magnetic correlations which are not liquid-like appear [6]. A steep increase of the Tb^{3+} magnetic moment μ_{Tb} and correlation length L_c is observed around $T_{\text{lr}} = 0.87$ K where a peak is seen in the temperature dependence of the specific heat $C_p(T)$. $\mu_{\text{Tb}} = 5.9(1) \mu_{\text{B}}$ with $L_c = 19$ nm at 0.10 K. Therefore, even far below T_{lr} , L_c is much shorter than usually observed in ordered magnetic structures.

We present below (i) $C_p(T)$ data recorded using a dynamic adiabatic technique, (ii) ND measurements carried out at the cold neutron powder diffractometer DMC of the SINQ facility at the Paul Scherrer Institute and (iii) μSR measurements done at the MuSR spectrometer of the ISIS facility (Rutherford Appleton Laboratory, Chilton, United Kingdom) and GPS and LTF spectrometers of the Swiss Muon Source (Paul Scherrer Institute, Villigen, Switzerland).

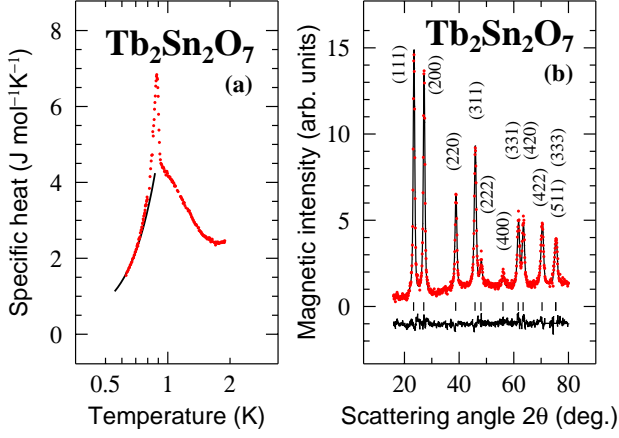


FIG. 1: (color online). (a). Low temperature dependence of the specific heat per mole of Tb measured for our $\text{Tb}_2\text{Sn}_2\text{O}_7$ sample. The sharp maximum is the signature of a magnetic transition occurring at $T_{\text{lr}} = 0.88$ K. The solid line is a fit to a model explained in the main text. (b). Magnetic powder diffraction pattern of $\text{Tb}_2\text{Sn}_2\text{O}_7$ versus the scattering angle 2θ obtained from the subtraction of data recorded at 0.11 K and 1.23 K. Neutrons of wavelength 2.453 Å were used. The solid lines show the best refinement and the difference spectrum (bottom). From the pattern analysis we extract a Tb^{3+} magnetic moment $\mu_{\text{Tb}} = 5.4(1) \mu_{\text{B}}$ which makes an angle of 14.2° with the local (111) axis. A measurement (not shown) at 0.98 K gives $\mu_{\text{Tb}} = 1.6(2) \mu_{\text{B}}$ and a Rietveld refinement of the diffraction pattern recorded at 100 K is consistent with space group $Fd\bar{3}m$ (lattice and oxygen position parameters equal to $a = 10.427$ Å and $x = 0.337$).

We first present $C_p(T)$ and powder ND measurements; see Fig. 1. Relative to the published $C_p(T)$ data [6], our sample displays a peak somewhat stronger in intensity at $T_{\text{lr}} = 0.88$ K. The magnetic ND pattern at low temperature is in very reasonable agreement with published results [6]. The magnetic reflections are not resolution limited and their tails are Lorentzian-like rather than the usual Gaussian-like. Their shape has been fitted in detail assuming a size distribution of sharply defined spherical magnetic domains. A magnetic reflection is then represented as the distribution-weighted sum of the peak profiles of domains of different sizes, each of them being convoluted with the instrument resolution function [14]. Two types of distributions, namely the log-normal and gamma distributions, were used for the fit of the data shown in Fig. 1b and gave similar results. For instance the average radii for the domains are 3.14 (10) and 2.95 (15) nm respectively for the two distributions. The volume-averaged domain diameter $D_v \equiv L_c$ can be deduced from the third and fourth moments M_3 and M_4 of the distribution using $D_v = 3M_4/(2M_3)$ [15]. Numerically, we find 19.8 and 19.1 nm for each of the considered distributions in excellent agreement with the value of L_c given above.

Now we report on the μSR data: see Refs. [16, 17]

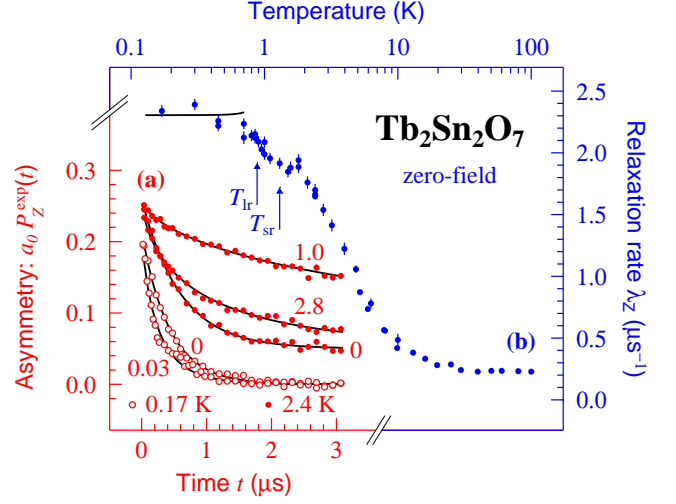


FIG. 2: (color online). (a). Two sets of μSR spectra recorded respectively at 0.17 and 2.4 K. For clarity the latter ones have been vertically shifted by 0.05. The numbers written next to each spectrum correspond to the longitudinal magnetic field, expressed in tesla, for which the data have been recorded. The solid lines are fits to the stretched exponential relaxation function, $P_Z^{\text{exp}}(t) = \exp[-(\lambda_Z t)^\alpha]$, where $\alpha = 1$ in zero-field. (b). Spin-lattice relaxation rate λ_Z versus temperature, deduced from spectra recorded using a cooling down sequence. The data were taken in zero-field, with the exception of some spectra above 4 K which were recorded in a longitudinal field $B_{\text{ext}} = 2$ mT. All the corresponding spectra were fitted with $\alpha = 1$. The solid line is deduced from the density of states introduced in the main text.

for an introduction to this technique. In Fig. 2a two zero-field spectra are presented, one recorded at a temperature $T > T_{\text{sr}}$ and a second deep in the ordered state i.e. $T \ll T_{\text{lr}}$. Unexpectedly, the two spectra are qualitatively similar, i.e. no clear-cut signature of the magnetic transition below T_{lr} is detected. We shall argue that this reflects the non-static character of the magnetic ground state of $\text{Tb}_2\text{Sn}_2\text{O}_7$.

We recall that the zero-field μSR technique gives access to the longitudinal polarization function $P_Z^{\text{exp}}(t)$ and, in the magnetically ordered state of a powder sample, it is expected to be the weighted sum of the longitudinal and transverse components: $P_Z^{\text{exp}}(t) = [\exp(-\lambda_Z t) + 2 \exp(-\lambda_X t) \cos(\gamma_\mu \langle B_{\text{loc}} \rangle t)]/3$. λ_Z and λ_X are, respectively, the spin-lattice and spin-spin relaxation rates, γ_μ is the muon gyromagnetic ratio ($\gamma_\mu = 851.615$ Mrad $\text{s}^{-1} \text{T}^{-1}$) and $\langle B_{\text{loc}} \rangle$ stands for the mean value of the local field at the muon site. Since all the measured spectra are exponential-like, this requires $\lambda_X \simeq \lambda_Z$ and the oscillatory behavior to be absent.

The first requirement is expected to be satisfied in the motional narrowing limit, i.e. when the dynamics of the Tb^{3+} moments is sufficiently fast; see for example Ref. [18]. The disappearance of the oscillations in the transverse component can have two origins: either

$\langle B_{\text{loc}} \rangle = 0$ or $\tau_c \ll (\gamma_\mu B_{\text{loc}})^{-1}$ where τ_c is the characteristic fluctuation time of B_{loc} . We consider now these two possibilities.

The local field is built up from the dipole fields generated by the Tb^{3+} magnetic moments. Taking into account the magnetic structure, we have mapped the dipole field in the unit cell. The computed field is small enough to be consistent with the experimental result only in the neighborhood of site (0.212, 0.537, 0.463) and symmetry equivalent sites. This site is located at $\simeq 1.4$ Å from the closest oxygen atom neighbor. This corresponds to a much larger distance than the one usually adopted by the muon site in oxides (range 1.0-1.1 Å) (see e.g. Refs. [19, 20]). Therefore this possibility is considered very unlikely.

Since the hypothesis $\langle B_{\text{loc}} \rangle = 0$ does not hold we now estimate a value of τ_c from our data. We assume for simplicity a transverse stochastic field jumping between two opposite orientations [21]. Generalization of this model would not change qualitatively the result. Referring to the spontaneous fields measured for $\text{Gd}_2\text{Ti}_2\text{O}_7$ [8] and $\text{Gd}_2\text{Sn}_2\text{O}_7$ [12], B_{loc} is estimated to be 0.2 T. Since with our model $\lambda_Z = \gamma_\mu^2 B_{\text{loc}}^2 \tau_c$, we compute $\tau_c = 8 \times 10^{-11}$ s from the measurements of λ_Z at low temperature (Fig. 2b). The whole μSR analysis is consistent since the motional narrowing condition is fulfilled ($\gamma_\mu B_{\text{loc}} \tau_c \simeq 0.01 \ll 1$).

Now we have to understand the observation of magnetic reflections in neutron scattering. The fact that these reflections can be indexed in the crystallographic structure of $\text{Tb}_2\text{Sn}_2\text{O}_7$ implies that the scattering is elastic or nearly elastic. The energy resolution of the DMC diffractometer given by the energy spread of the incident neutrons is $\Delta E = 0.4$ meV, a typical value for this kind of instrument. In other words, such a scattering experiment probes the magnetic structure with a time scale $\Delta t = \hbar/\Delta E = 1.6 \times 10^{-12}$ s. Since $\tau_c \gg \Delta t$ the ND and μSR results are compatible. Now, a time scale directly related to our diffraction measurements can be estimated. We use the relation $E = \hbar^2 k^2 / (2m_n)$ defining the energy of a neutron of wavevector k and mass m_n . From a momentum width of 0.04 Å^{-1} deduced from the average in \mathbf{k} space of the domain size distribution, a time scale of at most 2×10^{-10} s is obtained. It is rewarding that this value is of the same order of magnitude as τ_c .

Our result implies that the neutron scattering is not purely elastic, i.e. it occurs with a finite energy transfer. This dynamical order is consistent with the apparent reduction of the Tb^{3+} moment deduced from the nuclear specific heat relative to the neutron determination [6].

$\lambda_Z(T)$ is presented in Fig. 2b. The rate is first temperature independent from 100 K down to ~ 20 K and then starts to increase. This is consistent with the building up of pair-correlations at low temperatures [17]. λ_Z increases steadily as the sample is cooled. Remarkably, no sharp anomalies are detected at either T_{sr} or T_{lr} . $\lambda_Z(T)$

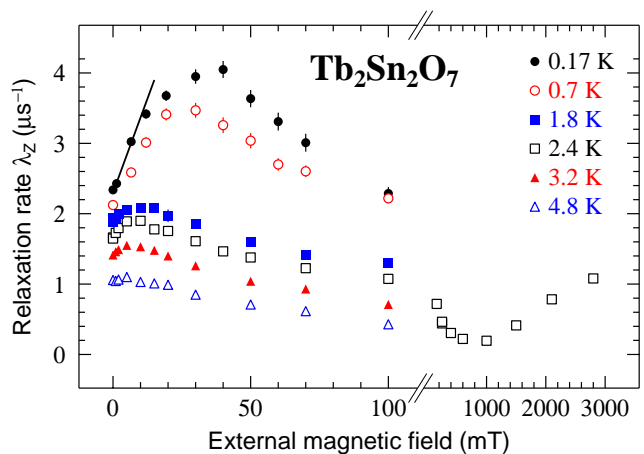


FIG. 3: (color online). Field dependence of λ_Z measured at low fields for $\text{Tb}_2\text{Sn}_2\text{O}_7$ using an experimental protocol explained in the main text. An amazing initial increase of λ_Z is observed at 3.2 K, i.e. far above T_{sr} , and down to 0.17 K. The shooting up of λ_Z at high field displayed for $T = 2.4$ K is also quite unexpected. The full line specifies the initial slope at 0.17 K which is $0.11 \mu\text{s}^{-1}\text{mT}^{-1}$.

presents an inflection point around T_{lr} . T_{sr} seems to correspond to a change in the slope of $\lambda_Z(T)$. Below 0.7 K λ_Z is observed to be only weakly temperature dependent down to the lowest measured temperature. That thermal behavior will be further discussed below.

We have also recorded μSR spectra under longitudinal fields (see Fig 2a). Whereas the sequence of the measurements has no importance for $T > T_{\text{sr}}$, it matters for $T < T_{\text{sr}}$, suggesting some hysteresis. In the latter case, the present results were deduced from spectra obtained by first cooling the sample in zero field from $T > T_{\text{sr}}$ and then using a field-increase sequence for the recording. In contrast to the zero-field spectra, a stretched exponential function (see caption of Fig. 2) with $\alpha < 1$ is needed to fit these ones [22]. α (equal to 1 in zero-field) decreases smoothly with field to reach a value of respectively ~ 0.8 for $T > T_{\text{sr}}$ and ~ 0.7 for $T < T_{\text{sr}}$ at 40 mT and then keeps this value up to 100 mT. $\lambda_Z(B_{\text{ext}})$ is presented in Fig. 3. The observed initial increase at low fields is unexpected. The slope is large and of approximately the same value for the two temperatures probed below T_{lr} and is still detectable in the paramagnetic phase up to 3.2 K. Since λ_Z decreases at large fields for all the temperatures, an extremum takes place at intermediate fields for $T \leq 3.2$ K. Its position is located around 5 mT at 3.2 K and goes up smoothly to reach a value ~ 40 mT at 0.17 K, i.e. almost an increase of an order of magnitude for more than a decade of temperature variation. The extremum being observed both in the ordered and paramagnetic states cannot originate from the response of magnetic domains or domain walls to B_{ext} .

The presence of such an extremum in $\lambda_Z(B_{\text{ext}})$ has

not been reported so far. The conventional Bloch-Wangsness-Redfield theory, which is expected to be valid at least for a temperature sufficiently large relative to T_{lr} , as at 3.2 K, predicts a monotonous decrease of $\lambda_Z(B_{\text{ext}})$ as B_{ext} is increased [18]. In addition, even if the low field part of the data is discarded, such a description breaks down because preliminary measurements, see Fig. 3, indicates $\lambda_Z(B_{\text{ext}})$ to shoot up at large fields, that is, above 1.0 T at 2.4 K. Note that this effect is not due to a change in α since $\alpha \approx 2/3$ for all fields from 0.4 T upwards.

We shall now provide a discussion for the λ_Z and C_p behaviors. As usual for geometrically frustrated magnetic materials, λ_Z is only weakly temperature dependent in zero-field at low temperature. This is accounted for by a Raman scattering process involving two magnetic excitations with a density of magnetic states characterized by an upturn at low energy and a small gap Δ proportional to the temperature [8], i.e. $\Delta = ak_{\text{B}}T$. A simultaneous fit of both $\lambda_Z(T)$ and $C_p(T)$ in the ordered state can be obtained using the density of states $g_m(\epsilon) = b_\mu \epsilon^{-1/2} + b_{\text{sh}} \epsilon^{5/2}$ for $\epsilon > \Delta$, where the first term gives rise to a temperature independent λ_Z and the second term has been chosen to reproduce our experimental $T^{7/2}$ dependence in $C_p(T)$. In Figs. 1a and 2b are shown the results of this model with $a = 0.02$ and b_μ and b_{sh} respectively equal to $0.057 \text{ meV}^{-1/2}$ and $73 \text{ meV}^{-7/2}$ per Tb atom. In addition we take the spectroscopic factor $g = 2$ and the anisotropy and exchange fields equal to $B_e = 10 \text{ T}$ and $B_a = 5 \text{ T}$, respectively (see Eq. 1 of Ref. 8). In fact, since, with the assumption $a \lesssim 1$, $\lambda_Z \propto b_\mu^2/a^2$, any set of a and b_μ parameters satisfying $b_\mu/a \simeq 3 \text{ meV}^{-1/2}$ will equally fit the data. The specific heat imposes a constraint: if b_μ is too large the first term in the density of states gives a contribution to $C_p(T)$. Therefore our combined set of data enforces $b_\mu \lesssim 0.06 \text{ meV}^{-1/2}$ and hence $a \lesssim 0.02$.

The increase of λ_Z at low fields is a definite signature of a field induced increase of the density of excitations at low energy. Because of the relatively large Zeeman energy on the system compared to Δ , the effect of the closure of the gap by the field is negligible. Indeed, at $B_{\text{ext}} = 10 \text{ mT}$ the Zeeman energy is $3.1 \mu\text{eV}$ which is large in comparison to the computed value $< 1 \mu\text{eV}$ for the gap at 0.17 K. Experimentally, attributing the stronger relaxation at low field to an increase of b_μ and using the value of the slope from Fig. 3, for $T < T_{\text{lr}}$ we estimate the relative change of b_μ between 0 and 10 mT to be 0.21.

In conclusion, the magnetic order with a limited correlation length observed in $\text{Tb}_2\text{Sn}_2\text{O}_7$ is dynamical in nature and characterized by a time $\sim 10^{-10} \text{ s}$, much less than previously inferred [6] but in agreement with our analysis of the neutron results. This is about an order of magnitude longer than estimated for the analogous compound $\text{Tb}_2\text{Ti}_2\text{O}_7$ which does not order [23, 24]. Our result implies that the magnetic scattering of the neutrons is not purely elastic. Such a dynamical ground

state is believed to be at work in the heavy fermion superconductor UPt_3 [25]. A sharp change in the dynamics at the temperature where a strong specific heat anomaly is detected has already been reported for the pyrochlore compound $\text{Yb}_2\text{Ti}_2\text{O}_7$ which in contrast displays no magnetic reflections [26]. $\text{Tb}_2\text{Sn}_2\text{O}_7$ is a new case since both a specific heat peak and broadened magnetic reflections are detected at low temperature. Given the time range of the fluctuations, the moments are not as correlated as it was inferred previously [6]. Neutron spin-echo experiments may provide an independent signature of the dynamical nature of the ground state of $\text{Tb}_2\text{Sn}_2\text{O}_7$. This dynamics is related to the existence of an appreciable density of magnetic excitations at low energy. We have discovered that it can be increased by applying a small magnetic field.

We are grateful to P. Bonville and S. Pouget for useful discussions and S. Sosin for complementary specific heat measurements. P.C.M. Gubbens thanks the Dutch Scientific Organisation (NWO) for its financial support for the use of ISIS. This research project has been partly supported by the European Commission under the 6th Framework Programme through the Key Action: Strengthening the European Research Area, Research Infrastructures; contract no: RII3-CT-20030505925.

* On leave from CNR, Istituto di Cristallografia (CNR-IC), 70126 Bari, Italy.

- [1] J. Villain, Z. Phys. **33**, 31 (1979).
- [2] A. P. Ramirez, in *Handbook of Magnetic Materials*, edited by K. H. J. Buschow (Elsevier, 2001), vol. 13.
- [3] J. E. Greedan, C. R. Wiebe, A. S. Wills, and J. R. Stewart, Phys. Rev. B **65**, 184424 (2002).
- [4] J. R. Stewart, G. Ehlers, A. S. Wills, S. T. Bramwell, and J. S. Gardner, J. Phys.: Condens. Matter **16**, L321 (2004).
- [5] J. D. M. Champion, M. J. Harris, P. C. W. Holdsworth, A. S. Wills, G. Balakrishnan, S. T. Bramwell, E. Cizmár, T. Fennell, J. S. Gardner, J. Lago, et al., Phys. Rev. B **68**, 020401(R) (2003).
- [6] I. Mirebeau, A. Apetrei, J. Rodríguez-Carvajal, P. Bonville, A. Forget, D. Colson, V. Glazkov, J. P. Sanchez, O. Isnard, and E. Suard, Phys. Rev. Lett. **94**, 246402 (2005).
- [7] A. S. Wills, M. E. Zhitomirsky, B. Canals, J. P. Sanchez, P. Bonville, P. Dalmas de Réotier, and A. Yaouanc, J. Phys.: Condens. Matter **18**, L37 (2006).
- [8] A. Yaouanc, P. Dalmas de Réotier, V. Glazkov, C. Marin, P. Bonville, J. A. Hodges, P. C. M. Gubbens, S. Sakarya, and C. Baines, Phys. Rev. Lett. **95**, 047203 (2005).
- [9] X. G. Zheng, H. Kubozono, K. Nishiyama, W. Higemoto, T. Kawae, A. Koda, and C. N. Xu, Phys. Rev. Lett. **95**, 057201 (2005).
- [10] J. Lago, T. Lancaster, S. J. Blundell, S. T. Bramwell, F. L. Pratt, M. Shirai, and C. Baines, J. Phys.: Condens. Matter **17**, 979 (2005).
- [11] E. Bertin, P. Bonville, J.-P. Bouchaud, J. A. Hodges,

- J. P. Sanchez, and P. Vulliet, Eur. Phys. J. B **27**, 347 (2002).
- [12] P. Bonville, J. A. Hodges, E. Bertin, J.-P. Bouchaud, P. Dalmas de Réotier, L.-P. Regnault, H. M. Rønnow, J.-P. Sanchez, S. Sosin, and A. Yaouanc, Hyperfine Interactions **156-157**, 103 (2004).
- [13] K. Matsuhira, Y. Hinatsu, K. Tenya, H. Amitsuka, and T. Sakakibara, J. Phys. Soc. Jpn **71**, 1576 (2002).
- [14] A. Cervellino, C. Giannini, A. Guagliardi, and M. Ladisa, Phys. Rev. B **72**, 035412 (2005).
- [15] N. C. Popa and D. Balzaral, J. Appl. Crystallogr. **35**, 338 (2002).
- [16] P. Dalmas de Réotier and A. Yaouanc, J. Phys.: Condens. Matter **9**, 9113 (1997).
- [17] P. Dalmas de Réotier, P. C. M. Gubbens, and A. Yaouanc, J. Phys.: Condens. Matter **16**, S4687 (2004).
- [18] C. P. Slichter, *Principles of Magnetic Resonance* (Springer, Berlin, 1996).
- [19] J. H. Brewer, R. F. Kiefl, J. F. Carolan, P. Dosanjh, W. N. Hardy, S. R. Kreitzman, Q. Li, T. M. Riseman, P. Schleger, H. Zhou, et al., Hyperfine Interactions **63**, 177 (1990).
- [20] B. Hitti, P. Birrer, K. Fischer, F. N. Gygax, E. Lippelt, H. Maletta, A. Schenck, and W. Weber, Hyperfine Interactions **63**, 287 (1990).
- [21] K. W. Kehr, G. Honig, and D. Richter, Z. Phys. B **32**, 49 (1978).
- [22] A slight deviation from the stretched-like behaviour has been detected at 0.17 K, with the maximum effect for the 70 mT spectrum. It manifests itself as a small shoulder between $\sim 0.1 - 0.3 \mu\text{s}$. We believe it could reflect the effect of a residual parasitic phase which can be hardly detected with powder X-ray scattering.
- [23] J. S. Gardner, S. R. Dunsiger, B. D. Gaulin, M. J. P. Gingras, J. E. Greedan, R. F. Kiefl, M. D. Lumsden, W. A. MacFarlane, N. P. Raju, J. E. Sonier, et al., Phys. Rev. Lett. **82**, 1012 (1999).
- [24] The sharp peak in the specific heat observed for crystals of $\text{Tb}_2\text{Ti}_2\text{O}_7$ at 0.37 K [27] is not a signature of a phase transition. Our own unpublished data recorded on crystals of $\text{Tb}_2\text{Ti}_2\text{O}_7$ do not exhibit any anomaly in this temperature range.
- [25] R. Joynt and L. Taillefer, Rev. Mod. Phys. **74**, 235 (2002).
- [26] J. A. Hodges, P. Bonville, A. Forget, A. Yaouanc, P. Dalmas de Réotier, G. André, M. Rams, K. Królas, C. Ritter, P. C. M. Gubbens, et al., Phys. Rev. Lett. **88**, 077204 (2002).
- [27] N. Hamaguchi, T. Matsushita, N. Wada, Y. Yasui, and M. Sato, Phys. Rev. B **69**, 132413 (2004).